Taylor & Francis
Taylor & Francis Group

The semi-automated classification of acoustic imagery for characterizing coral reef ecosystems

B.M. Costa[a,b]* and T.A. Battista[a]

[a]US National Oceanic & Atmospheric Administration Biogeography Branch, Silver Spring, MD 20910, USA; [b]Consolidated Safety Services, Inc., Fairfax, VA 22030, USA (under NOAA contract no. DG133C07NC0616)

Coral reef habitat maps describe the spatial distribution and abundance of tropical marine resources, making them essential for ecosystem-based approaches to planning and management. Typically, these habitat maps have been created from optical and acoustic remotely sensed imagery using manual, pixel- and object-based classification methods. However, past studies have shown that none of these classification methods alone are optimal for characterizing coral reef habitats for multiple management applications because the maps they produce (1) are not synoptic, (2) are time consuming to develop, (3) have low thematic resolutions (i.e. number of classes), or (4) have low overall thematic accuracies. To address these deficiencies, a novel, semi-automated object- and pixel-based technique was applied to multibeam echo sounder imagery to determine its utility for characterizing coral reef ecosystems. This study is not a direct comparison of these different methods but rather, a first attempt at applying a new classification technique to acoustic imagery. This technique used a combination of principal components analysis, edge-based segmentation, and Quick, Unbiased, and Efficient Statistical Trees (QUEST) to successfully partition the acoustic imagery into 35 distinct combinations of (1) major and (2) detailed geomorphological structure, (3) major and (4) detailed biological cover, and (5) live coral cover types. Thematic accuracies for these classes (corrected for proportional bias) were as follows: (1) 95.7%, (2) 88.7%, (3) 95.0%, (4) 74.0%, and (5) 88.3%, respectively. Approximately half of the habitat polygons were manually edited (hence the name 'semi-automated') due to a combination of mis-classifications by QUEST and noise in the acoustic data. While this method did not generate a map that was entirely reproducible, it does show promise for increasing the amount of automation with which thematically accurate benthic habitat maps can be generated from acoustic imagery.

1. Introduction

Benthic habitat maps provide critical information about the extent and composition of marine resources, and are vital for communicating information about the distribution and abundance of species (Townsend 2000) to resource managers, scientists, and the public. For this study, benthic habitat mapping is defined as the delineation and attribution of the biological cover and geomorphological structure of distinct coral reef ecosystem features on the seafloor. Habitat maps describe the location of benthic habitat features,

---

*Corresponding author. Email: bryan.costa@noaa.gov

their physical composition, and the types of organisms that colonize them. They support an increasing number of landscape ecology and habitat connectivity studies (Kendall, Christensen, and Hillis-Starr 2003; Garza-Pérez, Lehmann, and Arias-González 2004; Grober-Dunsmore et al. 2007; Pittman et al. 2007; Kendall et al. 2011), and are an important tool for ecosystem-based management (Andréfouët 2008; Crowder and Norse 2008; Hoffman and Gaines 2008; Wabnitz et al. 2008; Hamel and Andréfouët 2010), including the process of coastal and marine spatial planning, as well as the design (Leslie et al. 2003) and evaluation (Friedlander, Brown, and Monaco 2007) of marine protected areas (MPAs).

Passive optical imagery is most frequently used to map coral reef habitats in exceptionally clear, shallow, tropical waters (Kendall et al. 2001; Battista, Costa, and Anderson 2007a; Battista, Costa, and Anderson 2007b), where low levels of turbidity allow sunlight to penetrate the full-water column. Acoustic sensors are often deployed to map and characterize areas where depth information is needed and/or where water is turbid or too deep for passive optical sensors. The multibeam echo sounders (MBESs), in particular, are increasingly being used because they provide spatially accurate and continuous bathymetry (i.e. depth) and backscatter (i.e. intensity) imagery. MBESs collect this information by transmitting multiple beams of sound several times a second, and then recording the time, angle, and amplitude of each return (Burdic 1991). The depth and intensity images generated by MBESs have been used to characterize the benthic biology and geology of tropical areas (Lundblad et al. 2006; Costa, Bauer, and Mueller 2011; Costa, Tormey, and Battista 2012).

The following general methods have been used to create benthic habitat maps from optical and acoustic imagery: (1) manual delineation and attribution; (2) pixel-based classification; and (3) object-based classification. The manual delineation and attribution requires a cartographer to visually digitize, interpret, and characterize habitats visible in remotely sensed imagery. Pixel-based methods use algorithms to classify each individual pixel in a remotely sensed image. Object-based methods use algorithms to partition remotely sensed imagery into polygons (representing the boundaries of distinct habitat features) by determining their location relative to other features on the reef or by grouping neighbouring pixels with similar spatial, spectral, and textual characteristics (e.g. size, shape, colour, and intensity). All of these methods have their own advantages and disadvantages. On the one hand, manual classification methods have been used to develop benthic habitat maps at multiple spatial scales with high thematic resolutions (i.e. up to 30 distinct habitat classes) and high (i.e. >85%) overall thematic accuracies (Kendall et al. 2001; Coyne et al. 2003; Battista, Costa, and Anderson 2007a; Battista, Costa, and Anderson 2007b; Prada, Appeldoorn, and Rivera 2008). However, this method is time consuming and subjective because the habitat map's spatial and thematic accuracy depends on the knowledge and skill of the cartographer. Pixel-based methods, on the other hand, are potentially efficient and objective ways to classify imagery and develop habitat maps. However, these methods have been shown to be sensitive to noise in the imagery, exclude spatial and textual information from the classification process, and produce single-scale benthic habitat maps often with low thematic resolutions (<7 distinct classes) and/or lower overall thematic accuracies (<80%) (Anderson, Reed, and Winn 2001; Maeder et al. 2002; Mishra et al. 2006; Weiss, Miller, and Rooney 2008). Object-based methods, finally, are also potentially efficient and objective ways to develop habitat maps using spatial and textual information at multiple spatial scales. Even though these methods have been shown to produce habitat maps with high overall thematic accuracies (>93%) (Lucieer 2008), currently they are often unable to produce habitat maps which also have high thematic resolutions (Lucieer 2008).

Given that each classification method has its own strengths and weaknesses, previous studies have attempted to combine these methods to mitigate their individual limitations and produce a singular, robust classification method. The majority of studies have used semi-automated object- and pixel-based classification approaches to develop terrestrial maps from optical imagery (de Kok, Schneider, and Ammer 1999; Dorren, Bernhard, and Seijmonsbergen 2003; Walter 2004; Drăguţ and Blaschke 2006; Yu et al. 2006). Fewer studies have used semi-automated approaches to develop benthic marine habitat maps from optical imagery (Green and Lopez 2007; Urbański, Mazur, and Janas 2009), and even fewer studies have applied semi-automated approaches to develop benthic habitat maps from the MBES imagery (Costa and Battista 2008). Of all the studies with accuracy assessments (AAs) mentioned earlier, none were successful in creating a map with both high thematic resolutions (>25 classes) and overall accuracies (>85%). Rather, the resulting maps had either high thematic resolutions (≥43 distinct classes) and low overall thematic accuracies (≤56%) (Yu et al. 2006) or low thematic resolutions (two to seven distinct habitat classes) and high overall thematic accuracies (≥83%) (Dorren, Bernhard, and Seijmonsbergen 2003; Green and Lopez 2007; Urbański, Mazur, and Janas 2009). While these thematic resolutions and accuracies may be acceptable for certain applications, they are not representative of those commonly used in many scientific and management applications (Mumby et al. 1997; Monaco, Christensen, and Rohmann 2001) and may reduce the effectiveness of certain management actions (e.g. establishing no-take areas based on essential fish habitat) or inhibit the achievement of specific conservation goals (e.g. protecting a certain percentage of coral reefs in a given area) (Leslie et al. 2003; Kendall and Miller 2008). Habitat maps with higher thematic resolutions and accuracies can also simultaneously address many different management needs because they contain added information that may be relevant and scalable to a wider array of issues in the marine environment (Crowder and Norse 2008). Furthermore, new management problems cannot always be anticipated (e.g. with respect to climate change), which makes extracting the maximum amount of information from the MBES imagery potentially important for being prepared to meet future needs of the coastal and marine management community.

Keeping these issues in mind, we sought to develop a new semi-automated technique that would overcome the shortcomings of the classification methods described earlier and increase the thematic resolution and overall thematic accuracy of habitat maps produced from acoustic imagery. This new, semi-automated technique uses a combination of principal component analysis (PCA) (Pearson 1901; Hotelling 1933), edge-based segmentation (Jin 2009), QUEST algorithms (Loh and Shih 1997), and manual interpretation to create a benthic habitat map. The goals of applying this new technique were to produce a habitat map (1) efficiently and more objectively; (2) with a high thematic resolution (≥35 distinct habitat classes (Table 1), including major and detailed geomorphological structure, biological cover, and live coral cover); and (3) with high overall thematic accuracies (>85%). The following three specific research questions were addressed in trying to meet these goals.

(1) What surfaces and attributes are important for classifying benthic habitats from the MBES imagery?
(2) What thematic map resolution and accuracy can this semi-automated method achieve when applied to the MBES imagery?
(3) How much of the habitat map required manual editing and how does image quality affect this semi-automated method's performance?

Table 1.   Thirty-five distinct habitat classes were identified using this new technique.

Number	Distinct habitat class
1	Aggregate Reef, Algae 50–<90%, Live Coral 0–<10%
2	Aggregate Reef, Algae 50–<90%, Live Coral 10–<50%
3	Aggregate Reef, Algae 90–100%, Live Coral 0–<10%
4	Aggregate Reef, Algae 90–100%, Live Coral 10–<50%
5	Aggregate Reef, Live Coral 50–<90%, Live Coral 50–<90%
6	Aggregated Patch Reefs, Algae 10–<50%, Live Coral 0–<10%
7	Aggregated Patch Reefs, Algae 50–<90%, Live Coral 0–<10%
8	Aggregated Patch Reefs, Algae 50–<90%, Live Coral 10–<50%
9	Aggregated Patch Reefs, Algae 90–100%, Live Coral 0–<10%
10	Aggregated Patch Reefs, Algae 90–100%, Live Coral 10–<50%
11	Individual Patch Reef, Algae 50–<90%, Live Coral 0–<10%
12	Individual Patch Reef, Algae 50–<90%, Live Coral 10–<50%
13	Individual Patch Reef, Algae 90–100%, Live Coral 0–<10%
14	Individual Patch Reef, Algae 90–100%, Live Coral 10–<50%
15	Pavement with Sand Channels, Algae 50–<90%, Live Coral 0–<10%
16	Pavement with Sand Channels, Algae 50–<90%, Live Coral 10–<50%
17	Pavement, Algae 10–<50%, Live Coral 0–<10%
18	Pavement, Algae 50–90%, Live Coral 0–<10%
19	Pavement, Algae 50–<90%, Live Coral 10–<50%
20	Pavement, Algae 90–100%, Live Coral 0–<10%
21	Pavement, Algae 90–100%, Live Coral 10–<50%
22	Rhodoliths with Scattered Coral and Rock, Algae 50–<90%, Live Coral 0–<10%
23	Rhodoliths with Scattered Coral and Rock, Algae 90–100%, Live Coral 0–<10%
24	Rhodoliths, Algae 10–<50%, Live Coral 0–<10%
25	Rhodoliths, Algae 50–<90%, Live Coral 0–<10%
26	Rhodoliths, Algae 90–100%, Live Coral 0–<10%
27	Rhodoliths, Seagrass 10–<50%, Live Coral 0–<10%
28	Rhodoliths, Seagrass 50–<90%, Live Coral 0–<10%
29	Sand with Scattered Coral and Rock, Algae 10–<50%, Live Coral 0–<10%
30	Sand with Scattered Coral and Rock, Algae 50–<90%, Live Coral 0–<10%
31	Sand with Scattered Coral and Rock, No Cover 90–100%, Live Coral 0–<10%
32	Sand, Algae 10–<50%, Live Coral 0–<10%
33	Sand, Algae 50–<90%, Live Coral 0–<10%
34	Sand, No Cover 90–100%, Live Coral 0 –<10%
35	Sand, Seagrass 90–100%, Live Coral 0 –<10%

These three questions sought to answer the larger question: can this semi-automated method successfully delineate and characterize benthic habitats from the MBES imagery? If so, this novel approach may provide a useful alternative to other semi-automated classification methods, and to the manual classification method for characterizing benthic habitats using the MBES imagery.

2. Methods

The first step in this process was to acquire and process the high-resolution MBES imagery (Section 2.2). Benthic habitats were characterized using this MBES imagery using a combination of object-based, pixel-based, and manual classification methods (Figure 1; Costa et al. 2009). Several surfaces were derived from this imagery to describe the topographic complexity of the seafloor in different ways. Habitats with low and high levels of topographic complexity were classified separately. The PCA was used to remove highly correlated information contained in the suite of topographic complexity surfaces (Section 2.3). A first draft benthic habitat map was generated using edge-detection algorithms to delineate seafloor features with distinct acoustic signatures in the PCA and backscatter surfaces separately (Section 2.4). Polygons with distinct acoustic signatures were visited in the field with underwater video cameras (Section 2.5.1). The resulting video information was used to train the QUEST algorithm to classify each habitat feature automatically delineated by the edge-detection algorithm into different geomorphological structure, biological cover, and live coral classes based on their associated spatial, spectral, and textual metrics (Section 2.5.2). The two classifications were appended together and manually edited to create a final seamless habitat map (Section 2.6).

2.1. Description of study site

The study site, Virgin Islands Coral Reef National Monument, is a MPA administered by the National Park Service that is located off the southern coast of St. John in the US Virgin Islands (Figure 2). This 51.4 km^2 MPA was established in January 2001 by Presidential proclamation because it – along with the Virgin Islands National Park – contains some of the most biologically rich and economically important coral ecosystems in US Caribbean waters (Zitello et al. 2009). In particular, these shallow (<30 m)-to-moderate (30–60 m) depth waters support a diverse and complex system of coral reefs, shoreline mangrove forests, and seagrass beds, utilized by several marine species (Zitello et al. 2009).

2.2. Data acquisition and processing: the MBES imagery

Approximately 90 km^2 of MBES imagery was acquired in the southern Virgin Island Coral Reef National Monument boundaries on two separate missions from 18 February 2004 to 5 March 2004 and 1 February 2005 to 12 February 2005. During both missions, seafloor depths between 14 and 55 m were mapped at survey speeds between 4–7 knots using a pole-mounted SeaBat 8101 extended range 240 kHz MBES (Teledyne Reson, Goleta, CA, USA). An MBES was used instead of a single-beam echo sounder because MBESs provide highly resolved and spatially complete images of the seafloor. Additionally, an MBES was used instead of a light detection and ranging (lidar) system because most lidar systems cannot collect data deeper than approximately 30 m (Pittman, Costa, and Wedding 2013). During both years, the Reson 8101 data were collected to meet International Hydrographic Organization (IHO) Order 1 standards (IHO 2008). The data collected in 2005 met these uncertainty standards. However, the MBES data collected in 2004 (Figure 2) did not meet these standards because the pole-mount and MBES head vibrated during acquisition, introducing noise into the data. For more information about these surveys, see the following data acquisition and processing reports for projects: NF-04-06-VI (Monaco and Rooney 2004) and NF-05-USVI (Battista and Lazar 2005).

The MBES bathymetry and the backscatter data were acquired as Reson 8101 .xtf and .gsf files. The MBES backscatter snippets (i.e. the full time series of backscatter returns
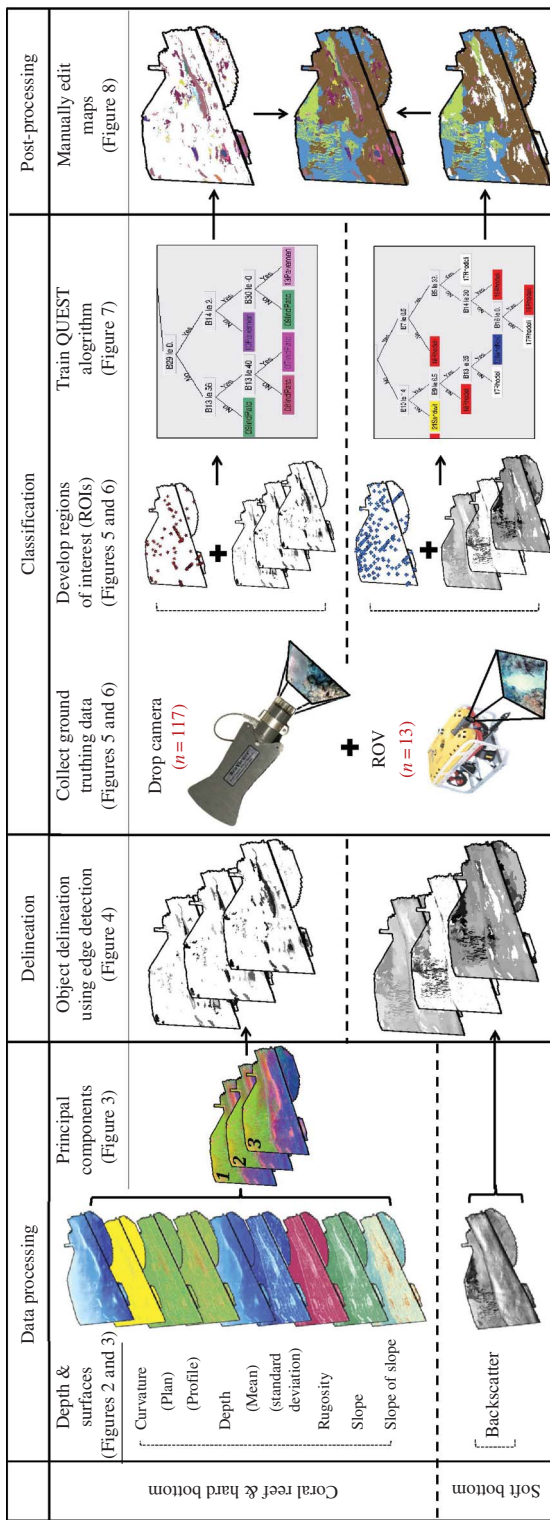
Figure 1.   Diagram illustrating the semi-automated process used to create the final benthic habitat map from the MBES imagery.
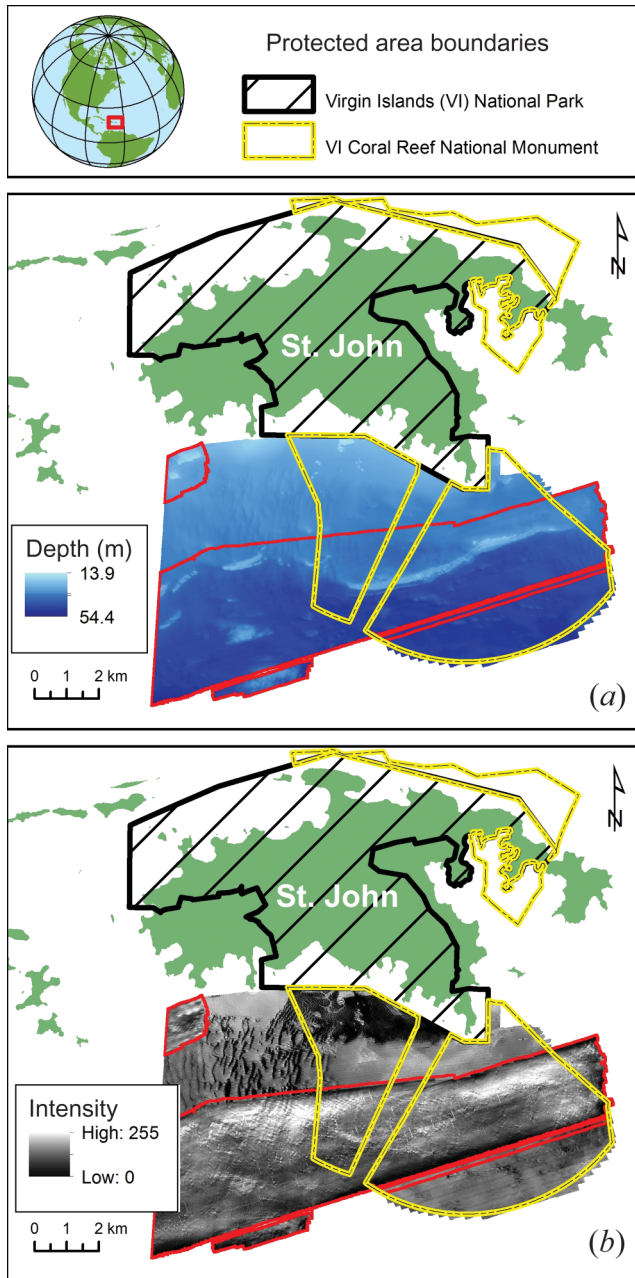
Figure 2. The US Virgin Islands (denoted by the inset box on the globe) includes St. Thomas, St. John, and St. Croix. The MBES data were collected south of St. John: (*a*) bathymetric imagery denoting the seafloor's depth in metres; and (*b*) backscatter imagery denoting the amount of sound returned from the seafloor. Backscatter intensity values do not have measurement units because they are relative (not absolute) numbers. The red polygons denote where the bathymetry did not meet IHO standards, and where the quality of the backscatter was degraded due to problems during the acquisition of the MBES data.

across a beam footprint) were geometrically and radiometrically corrected using Geocoder 3.0 software (Fonseca and Calder 2005; University of New Hampshire, Durham, NH, USA). The backscatter snippets were geometrically corrected for navigation attitude, transducer attitude, and local seafloor slope using the MBES bathymetric surface, and were radiometrically corrected for the changes in acquisition gains, power levels, pulse widths, incidence angles, and ensonification areas. All snippets were retained during these corrections, allowing the full resolution data to be used to create the final 16-bit, 2 × 2 m backscatter surface for the entire study area south of St. John.

CARIS software was used to clean and validate the MBES depth data (CARIS 2012; CARIS, Fredericton, Canada). Depths were corrected for sensor offsets, including roll, pitch, yaw, latency, static and dynamic draft, the changing speed of sound in the water column, and the influence of tides. Verified tide levels and tidal zoning files were supplied by NOAA's Center for Operational Oceanographic Products and Services. Erroneous soundings were removed manually. The 2004 and 2005 bathymetric surfaces were merged using ArcGIS's Raster Calculator to create a seamless 32-bit, 2 × 2 m bathymetry surface for the entire study area south of St. John.

2.3. Data processing: creating complexity surfaces

Eight topographic complexity surfaces were derived from the merged 2 × 2 m bathymetric surface. These surfaces specifically included (1) mean depth, (2) standard deviation of depth, (3) curvature, (4) plan curvature, (5) profile curvature, (6) rugosity, (7) slope, and (8) slope of slope (Figure 3; see Costa et al. 2009 for more details). Each of these surfaces was calculated in ArcGIS 9.2 (ESRI 2012; ESRI, Redlands, CA, USA) using a 3 × 3 cell neighbourhood, where the central pixel in the neighbourhood was assigned the calculated value. These eight surfaces were included in the classification process because previous studies demonstrated their utility for characterizing the distribution of coral reef ecosystems in the US Caribbean (Pittman, Costa, and Battista 2009).

Environment for Visualizing Images (ENVI) and ENVI Zoom 4.6 software, which are used to visualize, process, and analyse many types of remotely sensed imagery, were used to process these topographic complexity surfaces further (Exelis VIS 2012; Exelis Visual Information Solutions, Boulder, CO, USA). In ENVI 4.6, the bathymetry and the eight topographic complexity surfaces were subsequently rendered, stacked, and exported to create one image with nine different bands (i.e. each band representing a specific
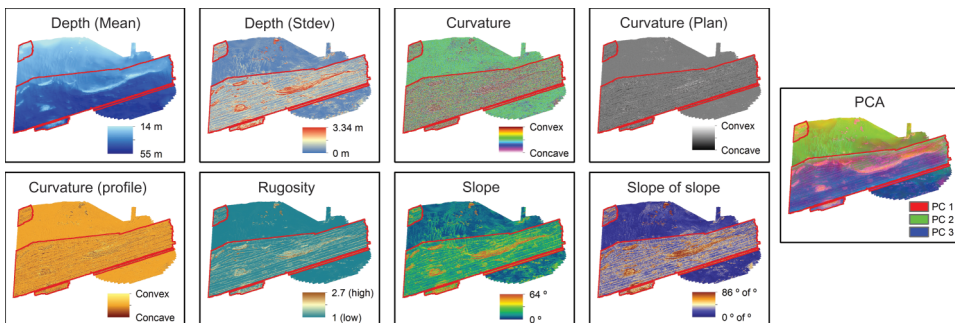

Figure 3.   Eight surfaces were used to create the PCA surface. These surfaces and PCA surface are pictured above. The red polygons denote where the bathymetry did not meet IHO standards, and where the quality of the backscatter was degraded due to problems during the acquisition of the MBES data.

topographic complexity surface). This image was then masked and transformed into its nine principal components (PCs) (based on the correlation). This transformation removed information that was highly correlated and thus, redundant across the different bands. The first three PCs were retained in the final image because they contained over 84% of the data variability uniquely describing the complexity and structure of the seafloor. These PCs were converted from 16-bit, floating point images to 8-bit, integer images, so that they could be imported into ENVI Zoom 4.6 for segmentation.

2.4. *Habitat map creation: seafloor feature delineation*

The ENVI Zoom 4.6 Feature Extraction (Fx) Module (Exelis VIS 2008) was used to segment the PCA and backscatter images separately using edge-detection algorithms developed by Jin (2009). These algorithms use a neighbourhood filter to identify the edges of real-world features in an image and assign pixels on either side of that edge to a single object (Glasbey and Horgan 1995). An object is defined as a group of pixels with similar spatial, spectral (brightness and colour), and/or textural characteristics that make it visually distinct from its surroundings (Exelis VIS 2008). Based on expert knowledge, features that appeared to be coral reef and hard bottom habitats (i.e. Aggregate Reef, Individual Patch Reefs, Aggregated Patch Reefs, Pavement, or Pavement with Sand Channels (see Costa et al. (2009) for more details)) were automatically delineated from the three-band PCA image. An attempt was made to automatically delineate these features from the original topographic complexity surfaces as well, but the segmented results using the PCA image were qualitatively much better. The hard bottom habitats were automatically delineated from the PCA image, and not the backscatter image, because the topographic complexity surfaces underlying the PCA made the vertical structure of coral reefs clearly visible. Based on expert knowledge, features that appeared to be soft bottom habitats (i.e. Sand or Sand with Scattered Coral and Rock, Rhodoliths or Rhodoliths with Scattered Coral and Rock) were automatically delineated from the backscatter image. These habitats were automatically delineated from the backscatter image because they lacked significant vertical structure and because backscatter is indicative of sediment properties not detected in the bathymetry surface, including grain size, and porosity (Hamilton et al. 1956; Shumway 1960; Hamilton 1972; Hamilton and Bachman 1982).

Three steps were involved in delineating discrete objects from an image (or images) using the ENVI Fx module: (1) segmenting the image, (2) merging smaller segments into larger objects, and (3) computing spatial, spectral, and textual attributes for each object. The first two steps are interactive and heuristic, allowing the analyst to incrementally adjust the input parameters to extract the features of greatest visual interest based on expert knowledge. In step 1, the 'scale level' of the edge-detection algorithm can be changed to decrease or increase the relative (not absolute) size of the objects to be extracted. Choosing a higher scale level (e.g. >75) causes a smaller number of larger segments to be defined, while choosing a lower scale level (e.g. <25) causes a greater number of smaller segments to be defined (Exelis VIS 2008). For this study, small adjustments were made to the scale parameter (in increments of five) and the effects of these changes were viewed in a preview window. The scale values that produced the best results in the preview window were selected heuristically. For coral reef and hard bottom habitats, a scale level of 75 was used to extract features because this value minimized the negative effect of noise in the PCA image on the segmentation process. A scale level of 25 was used to extract features that appeared to be soft bottom habitats because it minimized the negative effect of noise in the backscatter imagery on the edge-detection process.

In step 2, the 'merge level' of the algorithm can be modified to merge smaller segments into larger objects. Choosing a higher merge level (>75) causes segments with faded edges to be merged, while choosing a lower merge level (<25) preserves more of these features with faded edges (Exelis VIS 2008). For this study, small adjustments were made to the merge parameter (in increments of one) and the effects of these changes were viewed in a preview window. The scale values that produced the best results in the preview window were selected heuristically by sight. A merge level of 99.2 was used to merge features that appeared to be coral reef and hard bottom habitats in the PCA image, and a merge level of 99.1 was used to merge features that appeared to be soft bottom habitats in the backscatter surface. High merge levels were used in both segmentations to reduce the intra-class spectral and textual variance. The reduction of intra-class spectral and textual variance has been shown to increase the overall thematic accuracy of classified maps by up to 37% (Benfield et al. 2007; Wang, Sousa, and Gong 2004; Leech 2006; Yan et al. 2006).

In step 3, ENVI Fx computes 14 spatial metrics, four textual metrics, one band ratio metric, three hue/saturation/intensity metrics and four spectral metrics per input band for each distinct object. These different metrics (called Fx object attributes) are described in more detail in Exelis VIS (2008). After these Fx object attributes were calculated, all of the automatically delineated objects and attributes were exported from ENVI Fx as a single Environmental Systems Research Institute (ESRI) shapefile. Since coral reef features and soft bottom features were segmented individually, they were exported as separate shapefiles. The coral reef habitat shapefile had 34 attributes and 1287 polygons, whereas the soft bottom shapefile had 22 attributes and 11,421 polygons. In ArcGIS, each of the polygons and Fx object attributes were then converted to rasters using ArcGIS's 'Raster to Polygon' function. The resulting 34 coral reef rasters and 22 soft bottom rasters were stacked separately from each other, and exported to create two different images with several different bands (each band representing a specific Fx object attribute) (Figure 4). These two images were then classified using ground validation (GV) video and a supervised pixel-based approach to develop a final benthic habitat map.

2.5. *Habitat map creation: seafloor feature classification*

2.5.1. *Data acquisition and processing: ground validation video*

Extensive field work is needed to create benthic habitat maps with high thematic accuracies. Predetermined locations were visited to explore and verify habitats on the seafloor. These 'GV' locations were targeted to satisfy the following objectives: (1) explore features in the imagery with unknown acoustic signatures; and (2) confirm that the habitat type correlated with a particular acoustic signature remained consistent throughout the entire study area. Two different optical imaging systems were used to collect GV data in 2005 and 2009. Section 4 discusses the potential impact (on the habitat map) of the four-to-five-year time lag between the acquisition of the MBES imagery and some of the GV videos.

During the 2005 mission, GV data were collected from 1 February 2005 to 12 February 2005 along 13 transects between 1.5 and 3.5 km in length using a Spectrum Phantom S2 (Deep Ocean Engineering, San Leandro, CA, USA) remotely operated vehicle (ROV) (Figure 5) (Menza, Kendall, and Hile 2008). GV transects were arranged so as to intersect as many distinct acoustic signatures as possible. Video data were collected during an entire transect using a forward-looking camera, and still photographs were collected every 30 s using a downward-looking camera. The speed and height of ROV above the substrate were held constant at approximately 1 m s^{-1} and 2 m s^{-1}, respectively, to standardize the field of view and spatial resolution of interpretations. An Ultra Short Baseline system (ORE
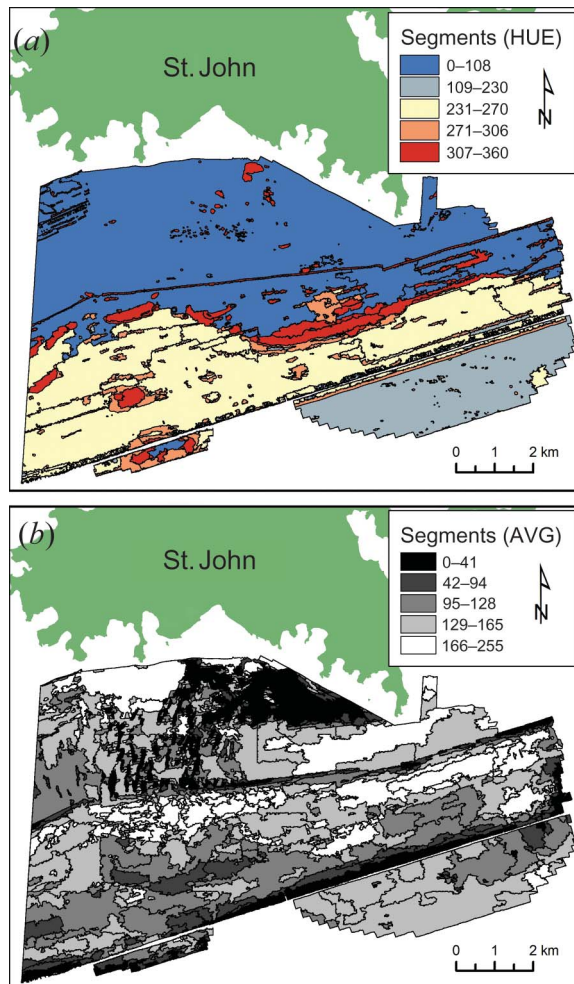
Figure 4. The PCA and backscatter surfaces were segmented separately. (*a*) Segments produced from the PCA surface symbolized using the 'HUE' attribute. (*b*) Segments produced from the backscatter surface symbolized using the 'AVG BAND' attribute. ENVI Zoom calculated 34 and 22 attributes for the segments produced from the PCA and backscatter, respectively.

Offshore, West Wareham, MA, USA) was used to determine the relative position of ROV to the ship.

During the 2009 mission, GV data were collected from 31 May 2009 to 7 June 2009 at 117 sites using an underwater drop camera (Figure 5). GV sites were systematically placed in parts of the study area that were not explored using the ROV. These GV sites were located using a hand-held Garmin 76 CS Wide Area Augmentation System (WAAS) enabled GPS unit (Garmin International, Inc., Olathe, KS, USA). Once onsite, the vessel's position was logged continuously using a Trimble GeoXT GPS receiver (Trimble Navigation Limited, Sunnyvale, CA, USA), and a SeaViewer Sea-Drop 950 camera (SeaViewer Underwater Video Systems, Tampa, FL, USA) was deployed to collect video of the seafloor. As the vessel drifted, the operator adjusted the camera to capture a downward and profile view approximately two metres above the seafloor. This consistent field of view was similar to the spatial resolution of the MBES imagery, and allowed for standardized measurements of percentage biological cover and broadscale understanding of the structure at each site.
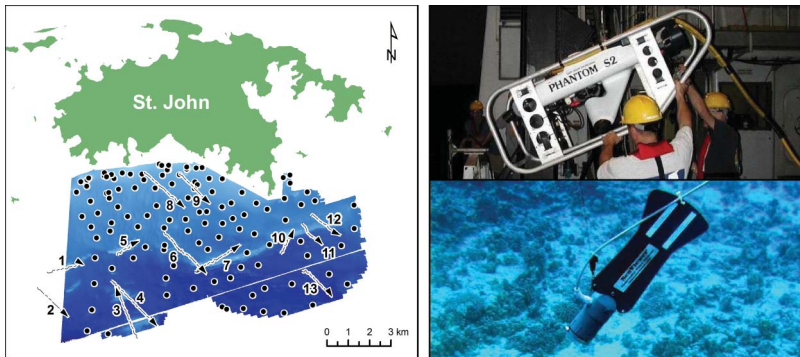
Figure 5. In 2005, the Spectrum Phantom S2 ROV (upper right) collected underwater video and high-resolution photographs of the seafloor along 13 transects for ground validation (GV) purposes. In 2009, the SeaViewer Sea-Drop 950 camera (lower right) collected underwater video of the seafloor at 117 discrete locations for GV purposes. The map (left) depicts these 13 transects and 117 locations overlaid on the bathymetric surface. The SeaViewer camera was also used for validation purposes.

Table 2. Different components of the habitat classification scheme, and how they are related to each other.

Geomorphological structure	Biological cover
Major structure	Major cover
Coral reef and hard bottom	*Algae*
Soft bottom	Live Coral
	Seagrass
Detailed structure	No Cover
Aggregate Reef	
Individual Patch Reef	Percentage major cover
Aggregated Patch Reefs	10–<50%
Pavement	50–<90%
Pavement with Sand Channels	90–100%
Rhodoliths	
Rhodoliths with Scattered Coral and Rock	Percentage live coral cover
Sand	0–<10%
Sand with Scattered Coral and Rock	10–<50%
	50–<90%

However, no attempt was made to standardize the amount of time the camera was on the seafloor. The layback between the camera and GPS antennae was estimated to be less than 25 m. The potential for mis-classifying habitats (due to the positional uncertainty introduced by layback) was minimized by targeting the centres of large homogeneous habitat polygons. The raw Trimble GPS data were post-processed and differentially corrected using the VITH Continually Operating Reference Station at St. Thomas, the US Virgin Islands.

The ROV and drop camera videos were visually classified into major and detailed geomorphological structure, major and detailed biological cover, and percentage live coral cover (Table 2). Habitat features were described by varying levels of detail (i.e. at the major and minor levels), so that users could refine the information depicted by the habitat map

to best suit their research and management needs. The biological cover class was assigned based on the dominant biological cover visible in the underwater video for each polygon. The live coral cover class included the presence of both hard and soft corals. More specifics about this classification scheme are described in Costa et al. (2009). The final classified GV points were then separated into multiple shapefiles (i.e. one file for each distinct habitat class). Each shapefile was subsequently imported into ENVI 4.6, and converted to regions of interest (ROIs). There were 2051 ROIs in total. The habitat classes that were more common and covered larger areas (e.g. Rhodoliths, Algae 90–100%, Live Coral <10%) had a higher number of ROIs than those classes that were less common and covered small areas on the seafloor (e.g. Individual Patch Reef, Algae 90–100%, Live Coral 10–50%).

2.5.2. *Data processing: training QUEST algorithm*

The ROIs created from the classified ROV and drop camera GV points were used to train the classification algorithm and to develop a final habitat map from the stacked Fx object attribute rasters. These tasks were performed using ENVI 4.6's Rule Gen 1.02 add-on (Jengo 2004). This add-on contains the QUEST algorithm (Loh and Shih 1997), which is implemented via ENVI's native Decision Tree Tool. QUEST is a type of Classification and Regression Tree (Breiman et al. 1984) that (1) is nonparametric and nonlinear, (2) has negligible variable selection bias, (3) is computationally simplistic, and (4) yields binary splits for categorical, ordinal or a mix of predictor variables (Figure 6). However, unlike Classification and Regression Trees, the QUEST algorithm separates objects in an image into classes using univariate (axis-orthogonal) discriminant-based splits. This type of analysis separates the classification process into two parts at each split (or node) in the decision tree.

The QUEST algorithm was used to classify each habitat object automatically delineated by ENVI Fx. Coral reef and soft bottom habitats were classified separately because they were delineated by Fx separately. ROIs for coral reef and soft bottom habitats each trained the QUEST algorithm to develop a classification tree. These two trees were built using the same input parameters (Costa et al. 2009), but different combinations of the spatial, spectral, textual, hue/saturation/intensity, and band ratio attributes. In total, the algorithm
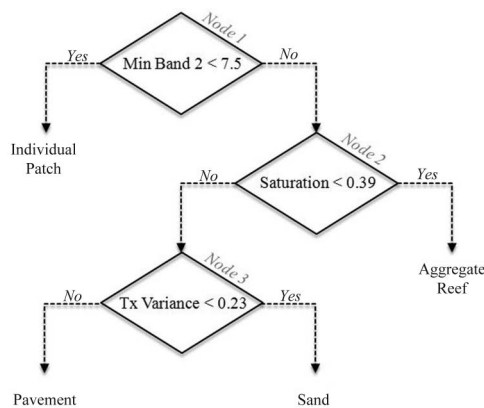
Figure 6.   This diagram illustrates how QUEST uses binary decisions to split an image into different classes. For example at node 1, if a habitat object's minimum band value is <7.5, it is attributed as 'Individual Patch Reef.' However, if a habitat object's minimum band value is ≥7.5, then QUEST advances to node 2 and so on down the line. While this example tree only has three nodes, the final coral reef and soft bottom decision trees had 91 and 71 nodes, respectively.

found 91 and 71 useful splits when grouping coral reef features, and soft bottom features, respectively. The final coral reef and soft bottom classifications were exported from ENVI 4.6 as separate ESRI shapefiles.

2.6. *Habitat map post-processing*

These ESRI shapefiles were imported into ArcGIS for additional post-processing and visual quality assurance and control. The first step in this process was to integrate the coral reef and soft bottom shapefiles into one single shapefile. To do so, all 698 of the coral reef polygons were spatially merged with the soft bottom shapefile using ArcGIS's Merge function. Next, we removed habitat polygons smaller than the 1000 m^2 minimum mapping unit (MMU). This MMU was chosen to be consistent with the adjacent shallow-water map for St. John (Zitello et al. 2009). Polygons smaller than the MMU were removed by merging them into neighbouring polygons with which they shared their longest common border using ET Geowizards (Tchoukanski 2008). The last post-processing step was to visually evaluate the appended map, and to edit polygons if necessary. These edits included re-classifying, merging or deleting polygons where the cartographer disagreed with the algorithm's interpretation. They also included manually digitizing habitat features (>1000 m^2 at a scale of 1:2000) that were not properly delineated during the feature extraction process due to the presence of acoustic noise. The end result was a seamless habitat map of the seafloor with 738 soft bottom polygons and 545 coral reef and hard bottom polygons.

2.7. *Habitat map evaluation: assessing the new semi-automated method's performance*

A statistically robust assessment of the habitat map's thematic accuracy was conducted. This assessment provided a quantitative understanding of the map's reliability (i.e. were certain habitats mis-classified?), and of the relationship between thematic resolution and accuracy (i.e. was the map too resolved to support high thematic accuracies?). It is important to note that this assessment was conducted by an independent scientist who was not involved with the development of the map.

Thematic accuracy was characterized for major and detailed geomorphological structure, major and detailed biological cover, and percentage live coral cover classifications. The accuracy of each of the 35 distinct habitat classes was not assessed independently because there was not enough money to do so. Target locations for the accuracy assessment were determined using a stratified random sampling technique to ensure that all bottom classifications were assessed. A minimum of 25 points were randomly placed within each detailed geomorphological structure class ($n = 225$) using Hawth's analysis tools (Beyer 2004). Seventy-four additional points were added to classes with larger areas. Underwater video was collected at each of these 299 sites between 31 May 2009 and 7 June 2009. The time lag between the acquisition of the MBES imagery and the validation drop camera videos may have impacted the accuracy of the classification results. This potential impact is discussed in more detail in Section 4. The same procedure that was used to collect and classify GV video was also used to collect and classify validation video (Section 2.5.1). The final classified validation points (n_i) were then spatially joined to the benthic habitat layer to extract the map classification for each point (n_j). The resulting attribute table was used to create five error matrices.

These error matrices were used to calculate the overall accuracy (P_o), producer's accuracy, and user's accuracy for the structure, cover, and live coral cover classes (Story and Congalton 1986). In addition to overall, producer's, and user's accuracies, these matrices were used to calculate the Tau coefficient (T_e) at the 95% confidence level ($1-\alpha$) (Ma and Redmond 1995). The Card (Card 1982) method was used to remove the bias introduced into the error matrices by unequal sampling rates (Hay 1979; Card 1982). This method utilizes map marginal proportions (π_j) to account for the disproportionate sampling of rare and common map categories. Map marginal proportions were calculated as the area of each map category (i.e. major and detailed geomorphological structure, major, and detailed biological cover) divided by the total area of the benthic habitat map. For example, the marginal proportion for Rhodoliths ($\pi_j = 0.77$) was calculated by dividing the class area (69.9 km^2) by the total map area (90.2 km^2). The map marginal proportions were also utilized in the computation of confidence intervals (CIs) for the overall, producer's, and user's accuracies (Card 1982; Congalton and Green 1999). Marginal proportions were not computed, however, for the percentage live coral cover matrix because the estimates of percentage hard bottom within each polygon needed to estimate the area of live coral were unavailable.

Another measure of this semi-automated method's performance was the ability of the combined object- and pixel-based algorithms to delineate and classify habitat features without any manual editing. Manual editing is defined as deleting, merging, adding or re-attributing habitat polygons that were classified by the computer. The total number of habitat polygons that were manually edited was estimated based on three iterations of randomly distributed points ($n = 5897$ total) created using the sampling design tool for ArcGIS (Menza and Buja 2008). These random points were stratified by unique habitat type (i.e. distinct combinations of detailed structure, detailed cover, and live coral cover) and weighted by area to prevent undersampling of rare habitat features. Each class was allocated a minimum of 25 points. Habitat classifications contained in the original map (i.e. the unedited map produced by QUEST) and the final map (i.e. the map which had its thematic accuracy assessed) were extracted at each of these points, and compared to determine whether the underlying polygon had been changed.

Based on the IHO standards and expert knowledge, specific areas in the source imagery were determined to be acoustically noisy and of poor quality. Further investigation showed that this noise was due to the pole-mount and MBES head persistently vibrating during data acquisition. This vibration occurred because the pole-mount flexed while surveying at 4–7 knots. This noise is most easily seen in the backscatter imagery (Figure 2) and the topographic complexity surfaces (Figure 3). The relationship between MBES image quality and the incorrect classification of habitat polygons was explored using Fisher's exact tests, chi-squared tests (with Yates continuity correction), and receiver operating characteristic area under curves (AUCs). Receiver operating characteristic AUCs were computed for each distinct geomorphological structure, biological cover, and live coral cover class. The Fisher's exact and chi-squared tests were used to further explore the relationship of MBES image quality and classification accuracy for 12 classes with relatively low thematic accuracies ($<80\%$). More specifically, the Fisher's exact tests were used for nine habitat classes that had (1) less than 25 validation points, (2) chi-squared expected values that were less than 1, and/or (3) more than 20% of the chi-squared expected values were less than 5. These classes included: Soft bottom, Aggregated Reef, Individual Patch Reef, Rhodoliths with Scattered Coral and Rock, Sand, Soft Bottom $<10\%$ Live Coral, No Cover, Algae 10–50%, and No Cover 90–100% habitats. The chi-squared test was used for the remaining three classes (i.e. Algae 50–90%, Algae 90–100%, and Hard

Bottom Live Coral 10–50%), which did not meet this criteria. The Yates continuity correction was applied because each class was represented by a 2×2 frequency table. Chi-squared tests (with Yates continuity correction) were also used to explore the relationship between MBES image quality and the number of polygons that were manually edited.

3. Results

3.1. *What surfaces and attributes are the most important for classifying coral reefs using the MBES imagery?*

The results from both PCA and QUEST algorithm were considered when examining which surfaces and attributes were important for classifying coral reef habitats. Depth, mean

Table 3. The amount (%) of variance contributed by a single complexity surface to each principal component (PC).

Surface	Units	Definition	PC 1	PC 2	PC 3	Total
			Percentage variance contributed			
Curvature	1/100 m	Rate of change in curvature across the surface highlighting ridges, crests, and valleys (in 3 × 3 cell neighbourhood)	0.11	10.92	0.01	11.04
Curvature (plan)	1/100 m	Curvature of the surface perpendicular to the direction of the maximum slope (in 3 × 3 cell neighbourhood)	0.11	9.19	0.00	9.30
Curvature (profile)	1/100 z units	Curvature of the surface parallel to the direction of the maximum slope (in 3 × 3 cell neighbourhood)	0.08	9.38	0.01	9.48
Depth	Metres	Water depth	0.56	0.04	10.50	11.09
Depth (mean)	Metres	Average water depth (in 3 × 3 cell neighbourhood)	0.56	0.03	10.50	11.09
Depth (standard deviation)	Metres	Dispersion of water depth values about the mean (in 3 × 3 cell neighbourhood)	9.47	0.08	0.10	9.65
Rugosity	Ratio value	Ratio of surface area to planar area (in 3 × 3 cell neighbourhood) (Jenness, 2002 and 2004)	6.06	0.04	0.33	6.43
Slope	Degrees	Maximum rate of change in slope (in 3 × 3 cell neighbourhood)	8.75	0.06	0.47	9.29
Slope of slope	Degrees of degrees	Maximum rate of maximum slope change (in 3 × 3 cell neighbourhood)	6.79	0.06	0.04	6.88
		Total	32.49	29.80	21.96	84.30

Notes: Approximately 84% of the variability in the data was contained in the first three principal components combined. See Costa et al. (2009) for more details about individual surfaces.

depth, and curvature were the most important surfaces for classifying coral reef habitats from MBES imagery because they explained the largest amount of variance in the combination of the first three PCs (Table 3). Variance in the first PC was explained primarily by standard deviation of depth, slope, rugosity, and slope of slope. Curvature, plan curvature, and profile curvature explained the majority of variance in the second PC, whereas depth and mean depth explained the majority of variance in the third PC. These patterns suggest that each topographic complexity surface contributed in a small way to the final classification, and should not be excluded from this process. The same is true for the backscatter surface because it provides information about the physical properties of the seafloor (Hamilton et al. 1956; Shumway 1960; Hamilton 1972; Hamilton and Bachman 1982), which are not contained in, or highlighted by, the topographic complexity surfaces. The backscatter surface was excluded from the PCA analysis because the noise present in the data would have been mistaken for unique information about the seafloor, which would have disproportionately affected each PC (Joliffe 2002) and most likely decreased the thematic accuracy of the final classification.

The Fx object attributes that were important to the classification process differed between coral reef habitats and soft bottom habitats. In particular, QUEST found that 19 ENVI Fx object attributes were useful for splitting coral reef habitat features into 21 distinct classes. Fourteen ENVI Fx object attributes were useful for splitting soft bottom habitat features into 14 distinct classes (Table 4). Six of these Fx object attributes (i.e. AVG_BAND, MAINDIR, MAX_BAND, TX_ENTROPY, TX_MEAN, TX_VARIANCE) were useful for splitting both types of habitat features.

3.2. What thematic map resolution and accuracy can this semi-automated method achieve when applied to the MBES imagery?

This semi-automated technique partitioned the MBES image into 35 distinct combinations of major and detailed geomorphological structure, major and detailed biological cover, and live coral cover (Figure 7). Overall accuracies (corrected for proportional bias) were high for major geomorphological structure (95.7%) (Table 5), major biological cover (88.7%) (Table 6) and detailed geomorphological structure (95.0%) (Table 7), and live coral cover (88.3%) (Table 8). They were lower (>74.0%) for detailed biological cover (Table 9).

User's accuracies were high (>85%) for all categories in the major and detailed geomorphological structure classes, and low (56–70%) for 5 out of 12 of the major and detailed biological cover and live coral cover classes. This trend suggests a systematic inclusion of habitat polygons within the wrong biological cover type class. However, no such trend was apparent for the geomorphological structure classes. It is important to note that a biological class was most often confused with the class next to it on the percentage cover continuum, whereas geomorphological classes were confused about an equal number of times with habitats that were acoustically very similar and very different to them. Producer's accuracies, on the other hand, ranged widely (i.e. 14–100%) across all habitat classes. This indicates that, while there were problems with omitting polygons within specific classes, there was no systematic mis-classification of geomorphological or biological class types overall. Three habitat classes (i.e. Sand with Scattered Coral and Rock, Seagrass and Live Coral) were excluded from this analysis, because they were rare and did not have enough validation points to robustly assess their thematic accuracy.

Table 4. The polygon metrics (calculated by ENVI Fx) that were identified by QUEST considered to be significant for classifying coral reef and hard bottom habitats and soft bottom habitats. In total, 19 metrics were important for classifying coral reef habitats, and 14 metrics were used to classify the soft bottom habitats. Six of these metrics were important for classifying both habitat types.

Type of attribute	Number of attributes	Fx attribute	Important for classifying coral reef and hard bottom?	Important for classifying soft bottom?	Definition	Formula
Hue, saturation, and intensity	1	HUE	Yes	–	Hue is often used as a colour filter and is measured in degrees from 0 to 360. A value of 0 is red, 120 is green, and 240 is blue.	
	2	SATURATION	Yes	–	Saturation is often used as a colour filter and is measured in floating-point values that range from 0 to 1.0.	
	3	INTENSITY	Yes	–	Intensity often provides a better measure of brightness than using the AVGBAND spectral attribute. Intensity is measured in floating-point values from 0 to 1.0.	
Spectral	4	AVGBAND_1	Yes	Yes	Average value of the pixels comprising the region in band 1. This band is the backscatter for the soft bottom habitats, and the first principle component in the PCA image for the coral reef/hard bottom habitats.	
	5	AVGBAND_2	No	–	Average value of the pixels comprising the region in band 2. This band is the second principle component in the PCA image.	

6	AVGBAND_3	No	—	Average value of the pixels comprising the region in band 3. This band is the third principle component in the PCA image.
7	MAXBAND_1	Yes	Yes	Maximum value of the pixels comprising the region in band 1. This band is the backscatter for the soft bottom habitats, and the first principle component in the PCA image for the coral reef/hard bottom habitats.
8	MAXBAND_2	Yes	—	Maximum value of the pixels comprising the region in band 2. This band is the second principle component in the PCA image.
9	MAXBAND_3	Yes	—	Maximum value of the pixels comprising the region in band 3. This band is the third principle component in the PCA image.
10	MINBAND_1	No	Yes	Minimum value of the pixels comprising the region in band 1. This band is the backscatter for the soft bottom habitats, and the first principle component in the PCA image for the coral reef/hard bottom habitats.
11	MINBAND_2	Yes	—	Minimum value of the pixels comprising the region in band 2. This band is the second principle component in the PCA image.
12	MINBAND_3	Yes	—	Minimum value of the pixels comprising the region in band 3. This band is the third principle component in the PCA image.

Table 4. (*Continued*).

Type of attribute	Number of attributes	Fx attribute	Important for classifying coral reef and hard bottom?	Important for classifying soft bottom?	Definition	Formula
	13	STDBAND_1	No	Yes	Standard deviation value of the pixels comprising the region in band 1. This band is the backscatter for the soft bottom habitats, and the first principle component in the PCA image for the coral reef/hard bottom habitats.	
	14	STDBAND_2	No	–	Standard deviation value of the pixels comprising the region in band 2. This band is the second principle component in the PCA image.	
	15	STDBAND_3	No	–	Standard deviation value of the pixels comprising the region in band 3. This band is the third principle component in the PCA image.	
Other	16	BANDRATIO	Yes	–	Values range from −1.0 to 1.0. ENVI Fx computes a normalized band ratio between two bands, using the following equation: $(B2 - B1)/(B2 + B1 + eps)$, where eps is a small number to avoid division by zero.	
Spatial	17	AREA	No	Yes	Total area of the polygon, minus the area of the holes. Values are in map units.	

18	COMPACT	Yes	No	A shape measure that indicates the compactness of the polygon. A circle is the most compact shape with a value of 1/pi. The compactness value of a square is 1/2(sqrt(pi)).	= Sqrt (4 * AREA / pi) / outer contour length
19	CONVEXITY	No	Yes	Polygons are either convex or concave. This attribute measures the convexity of the polygon. The convexity value for a convex polygon with no holes is 1.0, while the value for a concave polygon is less than 1.0.	= length of convex hull / LENGTH
20	ELONGATION	No	No	A shape measure that indicates the ratio of the major axis of the polygon to the minor axis of the polygon. The major and minor axes are derived from an orientated bounding box containing the polygon. Square = 1 and Rectangle > 1.	= MAXAXISLEN / MINAXISLEN
21	FORMFACTOR	Yes	No	A shape measure that compares the area of the polygon to the square of the total perimeter. The form factor value of a circle is 1, and the value of a square is pi / 4.	= 4 * pi * (AREA) / (total perimeter)^2
22	HOLESOLRAT	No	Yes	The ratio of the total area of the polygon to the area of the outer contour of the polygon. The hole solid ratio value for a polygon with no holes is 1.0.	= AREA / outer contour area
23	LENGTH	No	No	The combined length of all boundaries of the polygon, including the boundaries of the holes. This is different than the MAXAXISLEN attribute. Values are in map units.	

(*Continued*)

B.M. Costa and T.A. Battista

Table 4. (*Continued*).

Type of attribute	Number of attributes	Fx attribute	Important for classifying coral reef and hard bottom?	Important for classifying soft bottom?	Definition	Formula
	24	MAINDIR	Yes	Yes	The angle subtended by the major axis of the polygon and the x-axis in degrees. The main direction value ranges from $0°$ to $180°$. $90°$ is north/south, and $0°$ to $180°$ is east/west.	
	25	MAJAXISLEN	No	Yes	The length of the major axis of an orientated bounding box enclosing the polygon. Values are map units of the pixel size. If the image is not georeferenced, then pixel units are reported.	
	26	MINAXISLEN	Yes	No	The length of the minor axis of an orientated bounding box enclosing the polygon. Values are map units of the pixel size. If the image is not geo-referenced, then pixel units are reported.	
	27	NUMHOLES	No	Yes	The number of holes in the polygon. Integer value.	
	28	RECT_FIT	Yes	No	A shape measure that indicates how well the shape is described by a rectangle. This attribute compares the area of the polygon to the area of the orientated bounding box enclosing the polygon. Rectangle $= 1$ and non-rectangle <1.	$= AREA\,/\,(MAXAXISLEN\,*\,MINAXISLEN)$

29	ROUNDNESS	No	Yes	A shape measure that compares the area of the polygon to the square of the maximum diameter of the polygon. The 'maximum diameter' is the length of the major axis of an orientated bounding box enclosing the polygon. Circle = 1 and square = 4/pi.	= 4 * (AREA) / (pi * MAXAXISLEN^2)
30	SOLIDITY	Yes	No	A shape measure that compares the area of the polygon to the area of a convex hull surrounding the polygon. The solidity value for a convex polygon with no holes is 1.0, and the value for a concave polygon is less than 1.0.	= AREA / area of convex hull
31	TX_ENTROPY	Yes	Yes	Average entropy value of the pixels comprising the region inside the kernel. ENVI Zoom computes entropy, in part, from the Max Bins in histogram preference.	
32	TX_MEAN	Yes	Yes	Average value of the pixels comprising the region inside the kernel.	
33	TX_RANGE	No	No	Average data range of the pixels comprising the region inside the kernel. A kernel is an array of pixels used to constrain an operation to a subset of pixels.	
34	TX_VARIANCE	Yes	Yes	Average variance of the pixels comprising the region inside the kernel.	

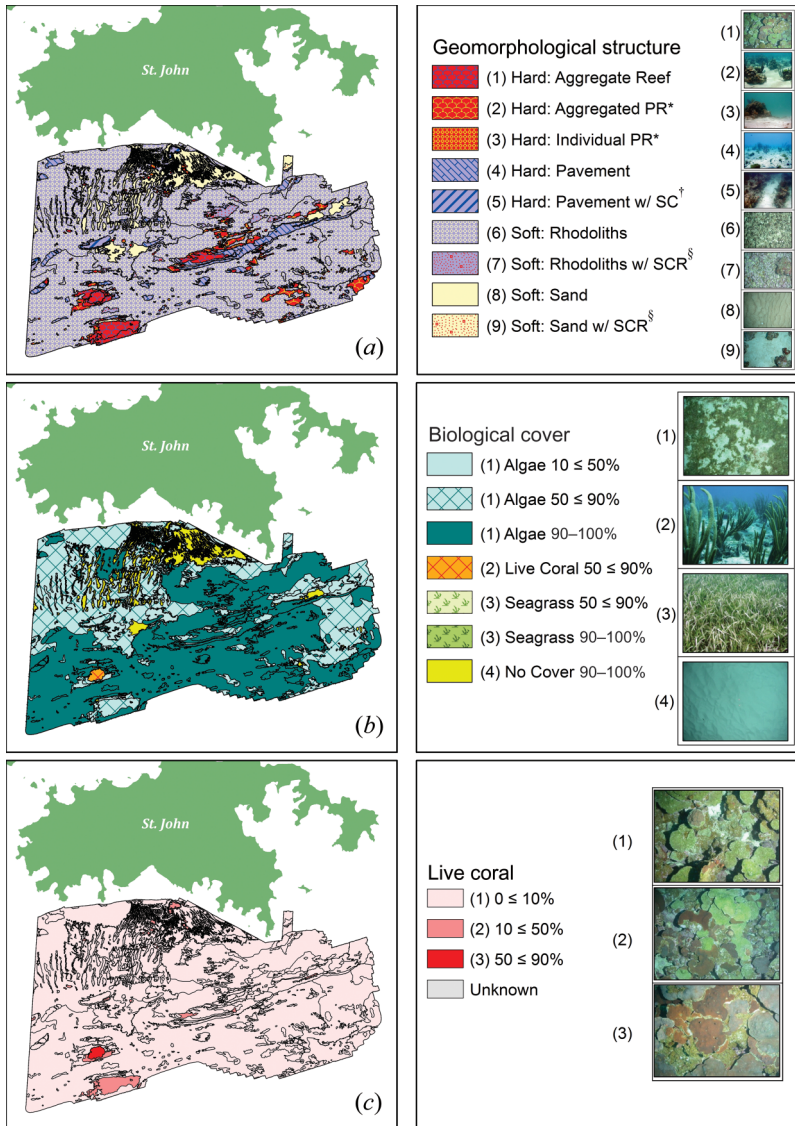Note: The symbol '-' denotes that the Fx metric was not calculated.

Figure 7. This figure depicts the final benthic habitat maps derived using the semi-automated classification method for (*a*) major and detailed geomorphological structure types; (*b*) major and detailed biological cover types; and (*c*) amount of hard and soft live coral cover.

Notes: *PR denotes 'patch reef,' †SC denotes 'sand channel,' and §SCR denotes 'scattered coral and rock'.

3.3. How much of the habitat map was manually edited and how did the quality of the MBES imagery affect the semi-automated method's performance?

The original map (i.e. the unedited map produced by QUEST) had a total of 1324 polygons that were larger than the map's MMU, whereas the final map (i.e. the map that had its thematic accuracy assessed) had a total of 1283 polygons. Approximately 55% of these polygons were manually edited (Table 10). Polygons that were edited manually occurred significantly more frequently in the area with low-quality imagery (i.e. which did

Table 5. Error matrix for major geomorphological structure.

Map data (j)	Accuracy assessment (i)			
	Hard bottom	Soft bottom	n_j	User's accuracy
Hard bottom	264 (154)	11 (6)	275 (160)	96.0%
Soft bottom	2 (1)	22 (1)	24 (2)	91.7%
n_i	266 (155)	33 (7)	$n = 299$	
Producer's accuracy	99.2%	66.7%	$P_o = 95.7\%$	
			$T_e = 0.913 \pm 0.046$	

Notes: The overall accuracy corrected for proportional bias is 95.7% ± 2.3; $\alpha = 0.05$. The values in parentheses denote the number of validation points located in areas with poor image quality.

Table 6. Error matrix for major biological cover. The overall accuracy corrected for proportional bias is 95.0% ± 2.3; $\alpha = 0.05$.

Map data (j)	Accuracy assessment (i)					
	No Cover	Live Coral	Algae	Seagrass	n_j	User's accuracy
No Cover	15 (1)		7 (0)		22 (1)	68.2%
Live Coral		1 (1)			1 (1)	—
Algae	7 (5)		269 (155)		276 (160)	97.5%
Seagrass				—	—	—
n_i	22 (6)	1 (1)	276 (155)	—	$n = 299$	
Producer's accuracy	68.2%	—	97.5%	—	$P_o = 95.3\%$	
					$T_e = 0.930 \pm 0.036$	

Note: The values in parentheses denote the number of validation points located in areas with poor quality imagery.

not meet IHO standards) than in the area with high-quality imagery (i.e. which did meet these standards) (chi-square (χ^2) = 14.01; degrees of freedom (df) = 1; $p \leq 0.0002$).

Not all habitat classes required equal amounts of editing. Detailed biological cover classes were the most frequently edited, followed by percentage biological cover, detailed geomorphological structure, major biological cover, major geomorphological structure, and live coral cover. For major structure, major cover, percentage cover, and live coral cover, significantly more polygons were edited in the areas that did not meet IHO standards ($\chi^2 = 6.489$; df = 1; $p \leq 0.01$; $\chi^2 = 6.63$; df = 1; $p \leq 0.01$; $\chi^2 = 9.15$; df = 1; $p \leq 0.003$; and $\chi^2 = 52.55$; df = 1; $p \leq 0.0001$, respectively). For detailed structure and detailed cover, equal numbers of polygons were edited in both areas ($\chi^2 = 0.02$; df = 1; $p \leq 0.90$ for the areas that met IHO standards and $\chi^2 = 1.16$; df = 1; $p \leq 0.28$ for areas that did not meet IHO standards).

4. Discussion

This novel semi-automated technique shows promise for characterizing coral reef ecosystems using MBES imagery, given the resulting habitat map's high thematic resolution (35 distinct combinations of structure and cover) and high thematic accuracies (>88% for major structure, major cover, detailed structure, and live coral cover classes). For our purposes, thematic resolutions ≥35 and accuracies >85% are both considered to be 'high' as defined in the introduction. It is important to emphasize that some applications (e.g.

designing biological sampling plans) may require fewer habitat classes and be able to tolerate higher levels of uncertainty, while others (e.g. assessing habitat damage from a ship grounding) may need higher thematic resolutions and accuracies than those presented here. These different requirements necessitate that resource managers and experts understand the limitations of the habitat map that they are using, and determine *a priori* the maximum amount of uncertainty allowed for their intended application.

While the overall thematic accuracies were high for most habitat types, this technique did have problems reliably identifying specific classes based on their user's and producer's accuracies ($<75\%$). For geomorphological structure, these class types included (1) Soft Bottom, (2) Aggregate Reef, (3) Individual Patch Reefs, (4) Rhodoliths with SCR, and (5) Sand. For biological and live coral cover, these class types included: (1) No Cover, (2) No Cover 90–$<$100%, (3) Algae 10–$<$50%, (4) Algae 50–$<$90% (5) Algae 90–100%, (6) Soft Bottom, Live Coral $<$10%, and (7) Hard Bottom, Live Coral 10–$<$50%. One possible explanation for these omission and commission errors (Congalton 1991) is the poor quality of the source imagery (i.e. the imagery that did not meet IHO standards) in some parts of the project area. The image quality was degraded in these areas because the pole on which the MBES transducer was mounted vibrated during data acquisition introducing errors into the bathymetry and noise into the backscatter. These artefacts, and the resulting low-quality imagery, affected the semi-automated classification method by making it difficult to distinguish among different habitat types. Polygons in the low-quality imagery areas required significantly more manual editing to remove acoustic noise, and were automatically delineated as distinct habitat features by the semi-automated method (Table 10). The same is true for percentage cover and live coral cover.

The low-quality imagery also reduced the user's and producer's thematic accuracies for certain classes automatically delineated and classified by the semi-automated method. This explanation is supported by the fact that there were significantly more validation points mis-classified in the low-quality imagery areas than in the high-quality imagery areas for the following classes: (1) Soft Bottom ($p \leq 0.002$), (2) Sand ($p \leq 0.001$), (3) Algae 50–90% ($\chi^2 = 10.04$; df $= 1$; $p \leq 0.002$; phi $= 0.27$), (4) Soft Bottom, Live Coral $<$10% ($p \leq 0.002$), and (5) Hard Bottom, Coral 10–50% ($p \leq 0.00005$). Additionally, low-quality imagery was found to be a reliable predictor of mis-classified validation points for the following classes: (1) Soft Bottom (AUC $= 0.75 \pm 0.15$), (2) Sand (AUC $= 0.78 \pm 0.17$), (3) Algae 50–90% (AUC $= 0.64 \pm 0.08$), (4) Soft Bottom, Live Coral $<$10% (AUC $= 0.75 \pm 0.15$), and (5) Hard Bottom, Coral 10–50% (AUC $= 0.82 \pm 0.11$). Thus, the low user's or producer's accuracies for these habitat classes were due to the poor quality of the imagery and not to the semi-automated classification technique itself.

For other habitat classes, however, poor image quality did not contribute to their lower ($<75\%$) thematic accuracies. These classes specifically included (1) Aggregate Reef, (2) Individual Patch Reefs, (3) Rhodoliths with Scattered Coral and Rock, (4) Algae 10–$<$50%, (5) Algae 90–100%, (6) No Cover, and (7) No Cover 90–$<$100%. This conclusion is supported by the fact that equal numbers of detailed structure and detailed cover polygons were edited in both low- and high-quality imagery areas (Table 10). Additionally, equal numbers of mis-classified validation points were located in the poor- and high-quality image areas ($p \leq 0.91$; $p \leq 1.0$; $p \leq 0.15$; $p \leq 0.95$; ($\chi^2 = 0.03$; df $= 1$; $p \leq 0.87$; phi $= 0.01$); $p \leq 0.07$; and $p \leq 0.07$, respectively), and poor image quality was not much better at predicting mis-classified validation points than random chance (AUC $= 0.6 \pm 0.27$; AUC $= 0.44 \pm 0.11$; AUC $= 0.77 \pm 0.35$; AUC $= 0.66 \pm 0.34$; AUC $= 0.51 \pm 0.07$; AUC $= 0.65 \pm 0.15$; AUC $= 0.65 \pm 0.15$, respectively). Thus, for these seven classes, other

Table 7. Error matrix for detailed geomorphological structure.

| Map data (*j*) | Accuracy assessment (*i*) | | | | | | | | | | |
	Aggregate Reef	Aggregated Patch Reefs	Individual Patch Reef	Pavement	Pavement with SC[†]	Rhodoliths	Rhodoliths with SCR[§]	Sand	Sand with SCR[§]	n_j	User's accuracy
Aggregate Reef	10 (7)		1 (0)							11 (7)	90.9%
Aggregated Patch Reefs		32 (20)	1 (0)	1 (1)		2 (2)	2 (2)			38 (25)	84.2%
Individual PatchReef			9 (1)							9 (1)	100.0%
Pavement	3 (3)	1 (1)	1 (0)	49 (35)		3 (2)		1 (1)		58 (42)	84.5%
Pavement with SC[†]	2 (0)				17 (8)					19 (8)	89.5%
Rhodoliths				4 (3)		117 (68)	1 (0)	7 (4)	3 (1)	132 (76)	88.6%
Rhodoliths with SCR[§]							8 (1)			8 (1)	100.0%
Sand						2 (1)		22 (1)		24 (2)	91.7%
Sand with SCR[§]									0 (0)	0 (0)	–
n_i	15 (10)	33 (21)	12 (1)	54 (39)	17 (8)	124 (73)	11 (3)	30 (6)	3 (1)	$n = 299$	
Producer's accuracy	66.7%	97.0%	75.0%	90.7%	100.0%	94.4%	72.7%	73.3%	–	$P_o = 88.3\%$	
											$T_e = 0.868 \pm 0.041$

Notes: The overall accuracy corrected for proportional bias is 88.7% ± 4.4; $\alpha = 0.05$. The values in parentheses denote the number of validation points located in areas with poor quality imagery.
[†]SC denotes 'Sand Channels'.
[§]SCR denotes 'Scattered Coral and Rock'.

Table 8. Error matrix for concatenated major geomorphological structure and percentage live coral cover. These numbers were not corrected for proportional bias because estimates of percentage hard bottom were not made for each polygon.

| | Accuracy assessment (i) | | | | | |
Map data (j)	Soft bottom, coral <10%	Hard bottom, coral <10%	Hard bottom, coral 10% ≤ 50%	Hard bottom, coral 50% ≤ 90%	n_j	User's accuracy
Soft bottom, coral <10%	22 (1)	2 (1)			24 (2)	91.7%
Hard bottom, coral <10%	11 (6)	219 (137)	5 (3)		235 (146)	93.2%
Hard bottom, coral 10% ≤ 50%		17 (12)	22 (1)		39 (13)	56.4%
Hard bottom, coral 50% ≤ 90%				1 (1)	1 (1)	–
n_i	33 (7)	238 (150)	27 (4)	1 (1)	$n = 299$	
Producer's accuracy	66.7%	92.0%	81.5%	–	$P_o = 88.3\%$ $T_e = 0.844 \pm 0.049$	

Note: The values in parentheses denote the number of validation points located in areas with poor quality imagery.

systematic biases caused the more frequent omission and commission errors, resulting in lower thematic accuracies.

One possible explanation for these lower thematic accuracies is that QUEST was unable to reliably classify these detailed structure and detailed biological cover classes. This explanation is supported by the fact that the detailed structure and detailed cover classes were not impacted by the quality of the MBES imagery, and yet they had the highest number of edited polygons out of any of the thematic habitat classes (Table 10). Future research that compares QUEST with different classification algorithms (e.g. boosted regression trees or random forest) would be useful to better understand this algorithm's limitations. In addition to the algorithm itself, some of the QUEST's mis-classifications may have occurred because a small number of ROIs used to train QUEST were mis-classified initially. ROIs may have been mis-classified because the amount of biological cover (particularly algae and seagrass) may have changed due to anthropogenic or environmental stressors and/or disturbances (Williams 1988) during the four-to-five-year time lag between the acquisition of the MBES imagery and validation videos. Also during that time, a mass-bleaching event (and subsequent disease) caused approximately 51.5% of the stony corals in the US Virgin Islands to die (Wilkinson and Souter 2008). One or both of these events may also explain the lower thematic accuracies of the four biological cover classes listed earlier.

However, it is unlikely that these events explain the lower thematic accuracies of the three detailed structure classes because geomorphological structure generally changes at much longer time scales than biological cover. ROIs for the remaining three detailed structure classes may have been mis-classified because they were located near the edges of habitat features, and were thought to be located in one habitat type, when in fact they were located in a different habitat type. This explanation is supported by fact that habitat classes with lower thematic accuracies had more ROIs near habitat boundaries than classes with higher thematic accuracies. For example, Aggregate Reef (producer's accuracy = 66.7%) had 47% of its ROIs located less than 25 m from a habitat boundary, whereas Rhodoliths (producer's accuracy = 94.4%) had only 23%. It is important to note that these two habitat

Table 9. Error matrix for detailed biological cover. The overall accuracy corrected for proportional bias is 74.0% ± 5.2; $\alpha = 0.05$.

Map data (j)	No Cover 90–100%	Live Coral 50–<90%	Algae 90–100%	Algae 50–<90%	Algae 10–<50%	Seagrass 90–100%	Seagrass 50–<90%	Seagrass 10–<50%	n_j	User's accuracy
No Cover 90–100%	15 (1)				7 (0)				22 (1)	68.2%
Live Coral 50–<90%		1 (1)							1 (1)	–
Algae 90–100%	3 (3)		127 (88)	45 (29)	6 (6)				181 (123)	70.2%
Algae 50–<90%	3 (2)		6 (5)	76 (24)	5 (1)				90 (32)	84.4%
Algae 10–<50%	1 (0)			1 (0)	3 (2)				5 (2)	60.0%
Seagrass 90–100%						–			–	–
Seagrass 50–<90%							–		–	–
Seagrass 10–<50%								–	–	–
n_i	22 (6)	1 (1)	133 (93)	122 (53)	21 (9)				$n = 299$	
Producer's accuracy	68.2%	–	95.5%	62.3%	14.3%				$P_o = 74.2\%$	
									$T_e = 0.678 \pm 0.062$	

Note: The values in parentheses denote the number of validation points located in areas with poor quality imagery.

Table 10. Estimated percentage of polygons at the 95% confidence interval (CI) that were re-attributed because they were manually deleted, added, edited, and/or merged in both high- and low-image-quality areas.

Class type	Estimated percentage of polygons that were edited	CI ($\pm$95%)	χ^2	df	p-Value $\leq$	More edited polygons in area with poor quality imagery
Major structure	$154/1283 = 12\%$	1%	6.49	1	0.0109	Yes
Detailed structure	$385/1283 = 30\%$	1%	0.02	1	0.8980	No significant difference
Major cover	$167/1283 = 13\%$	1%	6.63	1	0.0100	Yes
Percentage cover	$462/1283 = 36\%$	1%	9.15	1	0.0025	Yes
Detailed cover	$539/1283 = 42\%$	1%	1.16	1	0.2815	No significant difference
Live coral cover	$51/1283 = 4\%$	0%	52.55	1	0.0001	Yes
Distinct habitat class	$706/1283 = 55\%$	0%	14.01	1	0.0002	Yes

Note: Chi-squared (χ^2) test with Yates continuity correction (df = degrees of freedom) was used to determine whether significantly more of these edited polygons were located in areas with poor quality imagery.

classes had similar average sizes (i.e. 0.17 ± 0.24 km^2 and 0.16 ± 1.96 km^2, respectively) since ROIs are more likely to be located close to habitat boundaries in classes that cover less area (e.g. Individual Patch Reefs). To reduce the possibility of this error in the future, ROIs located near habitat transition zones should be removed from the training process to ensure their correct classification. Alternatively, ultrashort baseline acoustic tracking could be used to reduce the positional uncertainty associated with GV or validation point locations.

5. Conclusion

The new, semi-automated classification technique presented here created a thematically resolved and accurate benthic habitat map from MBES imagery, of which almost half of the polygons were delineated and classified by the computer alone. Even though this technique shows promise, more research is clearly needed to improve the reliable classification of specific habitats, and further reduce the amount of manual editing that is needed. Additionally, this method needs to be directly compared with other classification techniques to statistically determine whether it is capable of producing maps with similar thematic resolutions and accuracies. With further improvements, this semi-automated approach may be able to help to increase the efficiency with which benthic habitat maps are produced. Efficiently and accurately creating benthic habitat maps is the key to transforming the process of mapping from a static, resource inventory tool to a dynamic, resource monitoring tool. By doing so, resource managers would be able to more frequently assess the changes in the coral reef systems that they manage. Improving our understanding of these ecosystems is the key to identifying and mitigating the numerous threats faced by these resources in the present and future.

Acknowledgements

References

Anderson, A. J., T. B. Reed, and C. D. Winn. 2001. "Marine Sediment Classification Using Sidescan Sonar and Geographical Information System Software in Kaneohe Bay, Oahu, Hawaii." *Oceans Conference Record* 4: 2653–2657.

Andréfouët, S. 2008. "Coral Reef Habitat Mapping Using Remote Sensing: A User vs. Producer Perspective. Implications for Research, Management and Capacity Building." *Journal of Spatial Science* 53: 113–129.

Battista, T. A., B. M. Costa, and S. M. Anderson. 2007a. *Shallow-Water Benthic Habitats of the Republic of Palau*. NOAA Technical Memorandum NOS NCCOS 59, Biogeography Branch. Silver Spring, MD. Accessed March 14, 2013. http://ccma.nos.noaa.gov/products/biogeography/palau/htm/overview.aspx

Battista, T. A., B. M. Costa, and S. M. Anderson. 2007b. *Shallow-Water Benthic Habitats of the Main Eight Hawaiian Islands*. NOAA Technical Memorandum NOS NCCOS 61, Biogeography Branch. Silver Spring, MD. Accessed March 14, 2013. http://ccma.nos.noaa.gov/products/biogeography/hawaii_cd_07/

Battista, T. A., and J. V. Lazar. 2005. *MBES Data Acquisition and Processing Report: Project NF-05–05-USVI*: 1–74. NOAA Data Acquisition and Processing Report, NOS NCCOS CCMA. Accessed December 15, 2011. http://ccma.nos.noaa.gov/products/biogeography/usvi_nps/pdf/NF-05-05_DAPR.pdf

Benfield, S. L., H. M. Guzman, J. M. Mair, and J. A. T. Young. 2007. "Mapping the Distribution of Coral Reefs and Associated Sublittoral Habitats in Pacific Panama: A Comparison of Optical Satellite Sensors and Classification Methodologies." *International Journal of Remote Sensing* 28: 5047–5070.

Beyer, H. L. 2004. *Hawth's Analysis Tools for ArcGIS*. Accessed December 15, 2011. http://www.spatialecology.com/htools

Breiman, L., J. H. Friedman, R. A. Olshen, and C. J. Stone. 1984. *Classification and Regression Trees*, 1–358. Monterey, CA: Wadsworth and Brooks/Cole.

Burdic, W. S. 1991. *Underwater Acoustic System Analysis*, 1–466. 2nd ed. Los Altos, CA: Prentice Hall/Peninsula Publishing.

Card, D. H. 1982. "Using Known Map Categorical Marginal Frequencies to Improve Estimates of Thematic Map Accuracy." *Photogrammetric Engineering and Remote Sensing* 48: 431–439.

CARIS. 2012. "CARIS HIPS and SIPS Software Overview." Accessed March 14, 2013. http://www.caris.com/downloads/brochures/hipssips-en.pdf

Congalton, R. G. 1991. "A Review of Assessing the Accuracy of Classifications of Remotely Sensed Data." *Remote Sensing of Environment* 37: 35–46.

Congalton, R. G., and K. Green. 1999. *Assessing the Accuracy of Remotely Sensed Data: Principles and Practices*, 1–137. 2nd ed. Boca Raton, FL: CRC/Lewis Press.

Costa, B. M., and T. A. Battista. 2008. "Comparing Semi-Automated Methods for Classifying Multibeam SoNAR & Airborne LiDAR Imagery." In *Proceedings of the 11th International Coral Reef Symposium*, 667–671, Ft. Lauderdale, FL, July 7–11. Bayan Lepas: The WorldFish Center.

Costa, B. M., L. J. Bauer, T. A. Battista, P. W. Mueller, and M. E. Monaco. 2009. In *Moderate-Depth Benthic Habitats of St. John, U.S. Virgin Islands*, 1–72, Silver Spring, MD: NOAA Technical Memorandum NOS NCCOS 105. Accessed March 14, 2013. http://ccma.nos.noaa.gov/ecosystems/coralreef/benthic/StJohnModDepthRPTsm.pdf

Costa, B. M., L. J. Bauer, and P. W. Mueller. 2011. "Shallow-water Benthic Habitats of Jobos Bay." In *Baseline Assessment of the Resources of Jobos Bay, Puerto Rico*, edited by D. R. Whitall, B. M. Costa, L. J. Bauer, A. Dieppa, and S. D. Hile, 1–188, Silver Spring, MD: NOAA Technical Memorandum NOS NCCOS 133. Accessed March 14, 2013. http://ccma.nos.noaa.gov/publications/jobosbaybaseline.pdf

Costa, B. M., S. Tormey, and T. A. Battista. 2012. *Benthic Habitats of Buck Island Coral Reef National Monument*, 1–80. Silver Spring, MD: NOAA Technical Memorandum NOS NCCOS 142. Accessed March 14, 2013. http://ccma.nos.noaa.gov/ecosystems/coralreef/benthichabitats_buckisland.pdf

Coyne, M. S., T. A. Battista, M. Anderson, J. Waddell, W. Smith, P. Jokiel, M. S. Kendall, and M. E. Monaco. 2003. *Benthic Habitats of the Main Hawaiian Islands*, 1–49. Silver Spring, MD: NOAA Technical Memorandum NOS NCCOS CCMA 152, Biogeography Branch. Accessed March 14, 2013. http://ccma.nos.noaa.gov/products/biogeography/hawaii_cd/htm/manual.pdf

Crowder, L., and E. Norse. 2008. "Essential Ecological Insights for Marine Ecosystem-Based Management and Marine Spatial Planning." *Marine Policy* 32: 772–778.

de Kok, R., T. Schneider, and U. Ammer. 1999. "Object-based Classification and Applications in the Alpine Forest Environment." *International Achieves of Photogrammetry and Remote Sensing* 32: 1–7.

Dorren, L. K. A., M. Bernhard, and A. C. Seijmonsbergen. 2003. "Improved Landsat-based Forest Mapping in Steep Mountainous Terrain Using Object-based Classification." *Forest Ecology and Management* 183: 31–46.

Drăguţ, L., and T. Blaschke. 2006. "Automated Classification of Landform Elements Using Object-based Image Analysis." *Geomorphology* 81: 330–344.

ESRI (Environmental Systems Research Institute). 2012. "ArcGIS Overview." Accessed March 14, 2013. http://www.esri.com/software/arcgis/arcgis10

Exelis VIS (Visual Information Solutions). 2008. *ENVI Feature Extraction Module User's Guide*, 1–78. Accessed March 14, 2013. http://www.exelisvis.com/portals/0/pdfs/envi/Feature_Extraction_Module.pdf

Exelis VIS (Visual Information Solutions). 2012. *ENVI Overview*, 1–12. Accessed March 14, 2013. http://www.exelisvis.com/portals/0/pdfs/envi/Brochure_ENVI.pdf

Fonseca, L., and B. Calder. 2005. "Geocoder: An Efficient Backscatter Map Constructor." In *Proceedings of the U.S. Hydrographic Conference 2005*, March 29–31, 1–9. San Diego, CA: Hydrographic Society of America.

Friedlander, A. M., E. K. Brown, and M. E. Monaco. 2007. "Coupling Ecology and GIS to Evaluate the Efficacy of Marine Protected Areas in Hawaii." *Ecological Applications* 17: 715–730.

Garza-Pérez, J. R., A. Lehmann, and J. E. Arias-González. 2004. "Spatial Prediction of Coral Reef Habitats: Integrating Ecology with Spatial Modeling and Remote Sensing." *Marine Ecology Progress Series* 269: 141–152.

Glasbey, C. A., and G. W. Horgan. 1995. *Image Analysis for the Biological Sciences*, 1–188. Chichester: Wiley.

Green, K., and C. Lopez. 2007. "Using Object-Oriented Classification of ADS40 Data to Map the Benthic Habitats of the State of Texas." *Photogrammetric Engineering & Remote Sensing* 72: 665–675.

Grober-Dunsmore, R., T. K. Frazer, W. J. Lindberg, and J. Beets. 2007. "Reef Fish and Habitat Relationships in a Caribbean Seascape: The Importance of Reef Context." *Coral Reefs* 26: 210–216.

Hamel, M. A., and S. Andréfouët. 2010. "Using very High Resolution Remotes Sensing for the Management of Coral Reef Fisheries: Review and Perspectives." *Marine Pollution Bulletin* 60: 1397–1405.

Hamilton, E. L. 1972. "Compressional Wave Attenuation in Marine Sediments." *Geophysics* 37: 620–646.

Hamilton, E. L., and R. T. Bachman. 1982. "Sound Velocity and Related Properties of Marine Sediments." *The Journal of the Acoustical Society of America* 72: 1891–1904.

Hamilton, E. L., G. Shumway, H. W. Menard, and C. J. Shipek. 1956. "Acoustic and Other Physical Properties of Shallow-water Sediments off San Diego." *The Journal of the Acoustical Society of America* 28: 1–15.

Hay, A. M. 1979. "Sampling Designs to Test Land Use Map Accuracy." *Photogrammetric Engineering and Remote Sensing* 45: 529–533.

Hoffman, G. E., and S. D. Gaines. 2008. "New Tools to Meet New Challenges: Emerging Technologies for Managing Marine Ecosystems for Resilience." *BioScience* 58: 43–52.

Hotelling, H. 1933. "Analysis of a Complex of Statistical Variables into Principal Components." *The Journal of Educational Psychology* 24: 417–441.

IHO (International Hydrographic Organization). 2008. *IHO Standards for Hydrographic Surveys: Special Publication No. 44*. 5th ed. Accessed December 15, 2011. http://www.iho-ohi.net/iho_pubs/standard/S-44_5E.pdf

Jengo, C. 2004. *RuleGen 1.02 ENVI Tool*. Accessed March 14, 2013. http://www.exelisvis.com/UserCommunity/CodeLibrary.aspx

Jenness, J. 2002. *Surface Areas and Ratios from Elevation Grid*, Extension for ArcView 3.x version 1.2. Accessed March 14, 2013. http://www.jennessent.com/arcview/surface_areas.htm

Jenness, J. 2004. "Calculating Landscape Surface Area from Digital Elevation Models." *Wildlife Society Bulletin* 32: 829–839.

Jin, X. 2009. Segmentation-based image processing system. US Patent 20,090,123,070, filed November 14, 2007. Issued May 14, 2009. Accessed March 14, 2013. http://www.faqs.org/patents/app/20090123070

Joliffe, I. T. 2002. *Principal Component Analysis*, 1–487. 2nd ed. New York: Springer-Verlag.

Kendall, M. S., J. D. Christensen, and Z. Hillis-Starr. 2003. "Multi-scale Data Used to Analyze the Spatial Distribution of French Grunts, *Haemulon flavolineatum*, Relative to Hard and Soft Bottom in a Benthic Landscape." *Environmental Biology of Fishes* 66: 19–26.

Kendall, M. S., and T. Miller. 2008. "The Influence of Thematic and Spatial Resolution on Maps of a Coral Reef Ecosystem." *Marine Geodesy* 31: 75–102.

Kendall, M. S., M. E. Monaco, K. R. Buja, J. D. Christensen, C. R. Kruer, M. Finkbeiner, and R. A. Warner. 2001. *Methods Used to Map the Benthic Habitats of Puerto Rico and the U.S. Virgin Islands*. Silver Spring, MD: NOAA Biogeography Program. Accessed December 15, 2011. http://ccma.nos.noaa.gov/products/biogeography/usvi_pr_mapping/manual.pdf

Kendall, M. S., M. Poti, T. Wynne, B. Kinlan, and L. Bauer. 2011. "Ocean Currents and Larval Transport among Islands and Shallow Seamounts of the Samoan Archipelago and Adjacent Island Nations." In *A Biogegoraphic Assessment of the Samoan Archipelago*, edited by M. S. Kendall and M. Pot, 1–229. Silver Spring, MD: NOAA Technical Memorandum NOS NCCOS 132. Accessed March 14, 2013. http://ccma.nos.noaa.gov/ecosystems/coralreef/samoan_archipelago/samoabiogeorptfinalsm.pdf

Leech, M. J. 2006. "Comparison of Pixel-Based and Object-Oriented Approaches to Vegetation Mapping in Hawaii Using High Resolution IKONOS Imagery." M.S. thesis, Western Washington University, Bellingham, WA, 1–101.

Leslie, H., M. Ruckelshaus, I. R. Ball, S. Andelamn, and H. P. Possingham. 2003. "Using Siting Algorithms in the Design of Marine Reserve Networks." *Ecological Applications* 13: 185–198.

Loh, W.-Y. and Y.-S. Shih. 1997. "Split Selection Methods for Classification Trees." *Statistica Sinica* 7: 815–840.

Lucieer, V. L. 2008. "Object-oriented Classification of Sidescan Sonar Data for Mapping Benthic Marine Habitats." *International Journal of Remote Sensing* 29: 905–921.

Lundblad, E. R., D. J. Wright, J. Miller, E. M. Larkin, R. Rinehart, D. F. Naar, B. T. Donahue, S. M. Anderson, and T. Battista. 2006. "A Benthic Terrain Classification Scheme for American Samoa." *Marine Geodesy* 29: 89–111.

Ma, Z., and R. L. Redmond. 1995. "Tau Coefficients for Accuracy Assessment of Classification of Remote Sensing Data." *Photogrammetric Engineering and Remote Sensing* 61: 435–439.

Maeder, J., S. Narumainai, D. C. Rundquist, R. L. Perk, J. Schalles, K. Hutchins, and J. Keck. 2002. "Classifying and Mapping General Coral-Reef Structure Using IKONOS Data." *Photogrammetric Engineering and Remote Sensing* 68: 1297–1305.

Menza, C., and K. Buja. 2008. *Sampling Design Tool for ArcGIS*. Accessed March 13, 2013. http://ccma.nos.noaa.gov/products/biogeography/sampling/

Menza, C., M. Kendall, and S. Hile. 2008. "The Deeper We Go the Less We Know." *International Journal of Tropical Biology and Conservation* 56: 11–24.

Mishra, D., S. Narumaiani, D. Rundquist, and M. Lawson. 2006. "Benthic Habitat Mapping in Tropical Marine Environments Using Quickbird Multispectral Data." *Photogrammetric Engineering and Remote Sensing* 72: 1037–1048.

Monaco, M. E., J. C. Christensen, and S. O. Rohmann. 2001. "Mapping and Monitoring of U.S. Coral Reef Ecosystems." *Earth System Monitor* 12: 1–16.

Monaco, M. E., and S. C. Rooney. 2004. *MBES Data Acquisition and Processing Report: Project NF-04–06-VI*. NOAA Data Acquisition and Processing Report, NOS NCCOS CCMA. Accessed December 15, 2011. http://ccma.nos.noaa.gov/products/biogeography/usvi_nps/pdf/NF-04–06_DAPR.pdf

Mumby, P. J., E. P. Green, A. Y. Edwards, and C. D. Clark. 1997. "Coral Reef Habitat-mapping: How Much Detail Can Remote Sensing Provide?" *Marine Biology* 130: 193–202.

Pearson, K. 1901. "On Lines and Planes of Closest Fit to Systems of Points in Space." *Philosophical Magazine Series* 6: 559–572.

Pittman, S. J., C. Caldow, S. D. Hile, and M. E. Monaco. 2007. "Using Seascape Types to Explain the Spatial Patterns of Fish in the Mangroves of SW Puerto Rico." *Marine Ecology Press Series* 348: 273–284.

Pittman, S. J., B. M. Costa, and T. A. Battista. 2009. "Using LiDAR Bathymetry and Boosted Regression Trees to Predict the Diversity and Abundance of Fish and Corals." *Journal of Coastal Research* 53: 27–38.

Pittman, S. J., B. M. Costa, and L. M. Wedding. 2013. "LiDAR Application (Chapter 6)." In *Coral Reef Remote Sensing: A Guide for Mapping Monitoring and Management*, edited by J. A. Goodman, S. J. Purkis, and S. R. Phinn, 1–436. New York: Springer.

Prada, M. C., R. S. Appeldoorn, and J. E. A. Rivera. 2008. "Improving Coral Reef Habitat Mapping of the Puerto Rico Insular Shelf Using Side Scan Sonar." *Marine Geodesy* 31: 49–73.

Shumway, G. 1960. "Sound Speed and Absorption Studies of Marine Sediments by a Resonance Method." *Geophysics* 25: 451–467.

Story, M., and R. Congalton. 1986. "Accuracy Assessment: A User's Perspective." *Photogrammetric Engineering and Remote Sensing* 52: 397–399.

Tchoukanski, I. 2008. *ET Geo Wizards 9.8*. Extension for ArcGIS 9.2. Accessed December 15, 2011. http://www.ian-ko.com/

Townsend, P. A. 2000. "A Quantitative Fuzzy Approach to Assess Mapped Vegetation Classifications for Ecological Applications." *Remote Sensing of Environment* 72: 253–267.

Urbański, J. A., A. Mazur, and U. Janas. 2009. "Object-oriented Classification of Quickbird Data for Mapping Seagrass Spatial Structure." *International Journal of Oceanography and Hydrobiology* 38: 27–43.

Wabnitz, C. C., S. Andréfouët, D. Torres-Pulliza, F. E. Muller-Karger, and P. A. Kramer. 2008. "Regional-scale Seagrass Habitat Mapping in the Wider Caribbean Region Using Landsat Sensors: Applications to Conservation and Ecology." *Remote Sensing of Environment* 112: 3455–3467.

Walter, V. 2004. "Object-based Classification of Remote Sensing Data for Change Detection." *ISPRS Journal of Photogrammetry & Remote Sensing* 58: 225–238.

Wang, L., W. P. Sousa, and P. Gong. 2004. "Integration of Object-based and Pixel-based Classification for Mapping Mangroves with IKONOS Imagery." *International Journal of Remote Sensing* 25: 5655–5668.

Weiss, J., J. Miller, and J. Rooney. 2008. "Seafloor Characterization Using Multibeam and Optical Data at French Frigate Shoals, Northwestern Hawaiian Islands." In *Proceedings of the 11th International Coral Reef Symposium*, 662–666, Ft. Lauderdale, FL, July 7–11.

Wilkinson, C., and D. Souter. 2008. *Status of Caribbean Coral Reefs after Bleaching and Hurricanes in 2005*, 1–152. Townsville: Global Coral Reef Monitoring Network, and Reef and Rainforest Research Centre.

Williams, S. L. 1988. "Disturbance and Recovery of a Deep-water Caribbean Seagrass Bed." *Marine Ecology Progress Series* 42: 63–71.

Yan, G., J.-F. Mas, B. H. P. Maathuis, X. Zhang, and P. M. Van Dijk. 2006. "Comparison of Pixel-based and Object-oriented Image Classification Approaches – A Case Study in a Coal Fire Area, Wuda, Inner Mongolia, China." *International Journal of Remote Sensing* 27: 4039–4055.

Yu, Q., P. Gong, N. Clinton, G. Biging, M. Kelly, and D. Schirokauer. 2006. "Object-based Detailed Vegetation Classification with Airborne High Spatial Resolution Remote Sensing Imagery." *Photogrammetric Engineering & Remote Sensing* 72: 799–811.

Zitello, A. G., L. J. Bauer, T. A. Battista, P. W. Mueller, M. S. Kendall, and M. E. Monaco. 2009. *Shallow-water Benthic Habitats of St. John, U.S. Virgin Islands*, 1–68. Silver Spring, MD: NOAA Technical Memorandum NOS NCCOS 96, Biogeography Branch. Accessed March 14, 2013. http://ccma.nos.noaa.gov/ecosystems/coralreef/benthic/ShallowBenHabStJohn_Zitello_etal_reduced_qual.pdf